Vietnam Journal of Catalysis and Adsorption
Tạp chí xúc tác và hấp phụ Việt Nam

https://jca.edu.vn

Tuning Electronic Properties of Adsorbates on ZrO_2/Pt_3Zr Thin Films: A DFT Study

Ho Viet Thang*, Duong Thi Hong Phan, Nguyen Thi Minh Xuan

The University of Danang, University of Science and Technology, Danang 550000, Viet Nam
**Email: hvthang@dut.udn.vn*

ARTICLE INFO

Received: 15/2/2023
Accepted: 28/5/2023
Published: 30/3/2024

Keywords:
Adsorption; charge transfer; ZrO_2; ZrO_2/Pt_3Zr; DFT

ABSTRACT

We study the absorption of single atom Au and dissociation of H_2 molecule on ZrO_2 film deposited on Pt_3Zr surface using density functional theory (DFT) calculations including dispersion and U Hubbard correction. Parallel studies are also done for freestanding thin film ZrO_2 for comparison. Compared to unsupported ZrO_2 thin films, where only physical adsorption or unfavorable adsorption was observed, a completely different behavior is found for Au and H_2 adsorbed on ZrO_2/Pt_3Zr films. This is accompanied by clear changes in the electronic structure of the adsorbates. Analysis of the Bader charge, the spin density as well as the density of states clearly show that the main reason causing the significant difference in adsorption characteristics of Au and H_2 on ZrO_2/Pt_3Zr as compared to freestanding ZrO_2 thin film is the charge transfer at the interface of ZrO_2/Pt_3Zr.

1. Introduction

Metal oxide thin films deposited on metal support have been widely applied in many important fields, such as adsorption, catalysis, sensor, and electronic devices [1,2]. Due to the particular properties and tuning of the electronic characteristics of thin film deposited on metals, various metal oxide thin films have been synthesized successfully, for example, CeO_2/Pt(111) [3], ZnO/Au(111) [4], MgO/Mo(100) [5], ZrO_2/Pt(111) [6]. The main contribution leading to the difference in electronic properties of thin films deposited on metal support compared to freestanding ones is the effect of the metal support which can donate or accept electrons from atomic, molecular species adsorbed on the top of thin film. The charge transfer direction depends on the nature of metal support and thin films. For instance, the charge transfer from the metal support Mo to Au species occurred for Au adsorbed on MgO/Mo(100) thin film [7], while the charge transfer from Au atom to metal support was observed when Au adsorbed on FeO/Pt(111) thin films [8]. The electron flow takes place between support and adsorbed species through the tunneling mechanism. However, the electron tunneling depends on the thickness of the film, this phenomenon only occurs with a thin film thickness of less than 1 nm, beyond this thickness the electron transfer could not be observed. This means that the electronic properties of adsorbed species could not differ when adsorbing on metal oxide or supported metal oxide with a large thickness [9].

ZrO_2 material is extensively used in catalysis applications, especially in the hydrogenation of CO_2 molecules and biomass conversion into fuels [10,11]. In these applications, the dissociation of H_2 molecules plays an important role, and understanding these phenomena provides useful

https://doi.org/10.62239/jca.2024.009

information for the catalytic application of ZrO_2 in which H_2 is involved. Furthermore, tuning the electronic properties of ZrO_2 can be modified by changes in the structure size as nano or thin film within a thickness of a few nanometers. These materials can be obtained on different supports such as glass, metal, and alloy. Among these supports, the ZrO_2 thin film consisting of one trilayer O-Zr-O was obtained on alloy support $Pt_3Zr(0001)$ single crystal by oxidation of the surface Zr atoms which exhibits interesting properties in adsorption and catalysis [12,13]. However, the effect of metal support on the electronic characteristics of adsorbates is well established, while the role of alloy support Pt_3Zr on the electronic properties of ZrO_2 thin film and also adsorbed species are still missing.

In the present study, we theoretically investigated the effect of alloy Pt_3Zr supported thin film ZrO_2 on the electronic properties of adsorbed species consisting of single atom Au and H_2 molecules. To this end, we applied a PBE+U method, including dispersion force. The calculated results reveal that the electronic properties of adsorbed species on ZrO_2/Pt_sZr thin film are completely different from freestanding ultra-thin film ZrO_2.

2. Experimental

All calculations were performed applying spin-polarized density functional theory (DFT) with the Vienna Ab Initio Simulation Package [14,15]. The interaction between nuclei and core electrons was evaluated by Projector Augmented Wave (PAW) pseudopotentials [16]. The Generalized Gradient Approximation within Perdew–Burke–Ernzerhof (PBE) functional was used to describe the exchange-correlation functional [17]. To partly correct the self-interaction error of PBE functional, the PBE+U approach was applied as suggested by Dudarev et al. [18], in which an on-site Coulomb correction, U_{eff} = U – J = 4 eV was used for Zr 4d states [19]. Applying this PBE+U method, the calculated lattice parameters of bulk t-ZrO_2 are in good agreement with experimental parameters [20].

Particularly, the calculated (experimental) lattice parameters are a = b = 3.65 (3.64) Å and c = 5.21 (5.27) Å. Plane wave basis set with a kinetic energy cut-off of 400 eV and a 2 × 2 × 1 k-point grid were applied. All atoms were allowed to relax with ionic forces smaller than |0.01| eV $Å^{-1}$ and an electronic threshold of 10^{-5} eV.

Furthermore, the long-range dispersion forces in all calculations were considered by using Grimme (DFT-D2) scheme [21], in which the van der Waals radii (R0) and the C6 parameters for Zr cations were used the precedent noble gas in the periodic table (Kr), this is due to the size of Kr is closer to that of Zr^{4+} cations, thus denoted as DFT + D2' as suggested by Sergio et al. [22].

A monolayer (4 × 4) supercell with (101) orientation was adopted to model the freestanding ZrO_2 thin film, while this (4 × 4) supercell ZrO_2 thin film deposited on a 5-layer (3 × 3) supercell of the Pt-terminated (0001) Pt_3Zr surface was used to model the ZrO_2/Pt_3Zr structure. To avoid interactions between slabs, a vacuum thickness of 20 Å was constructed. Those models were described in detail in the previous study [19]. The adsorption energy of an Au and H_2 molecule was calculated as follows

$$E_{ads} = E(Ad/Support) – E(Support) – E(Ad)$$

where E(Ad/Support) is the energy of an adsorbed species (Au or H_2) on the support (unsupported ZrO_2 thin film or ZrO_2/Pt_3Zr), E(Support) is the energy of the support (unsupported ZrO_2 thin film or ZrO_2/Pt_3Zr), and E(Ad) is the energy of a free Au single atom or free H_2 molecule. The effective charges of atoms were obtained by applying the Bader method [23–25].

3. Results and Discussion

Au adsorption on freestanding ZrO_2 and ZrO_2/Pt_3Zr thin films

On freestanding ZrO_2 thin film, Au single atom can adsorb on three different sites, Zr-top, O-top, and hollow sites as illustrated in Fig 1. Among these sites, Au prefers to stabilize on the hollow site with an adsorption energy of -0.80 eV. At this configuration, Au bound to three O surfaces ad to three Zr surfaces with a distance of 2.66 Å and 3.18 Å, respectively (Table 1 and Fig 2a). The second most stable position for Au adsorption on freestanding ZrO_2 was found on Zr-top site with an adsorption energy of -0.77 eV. This is 0.03 eV smaller than on hollow site in magnitude. Compared to hollow site, Au bound to Zr with a smaller distance of 2.92 Å (Table 1 and Fig 2b). The

https://doi.org/10.62239/jca.2024.009

least stabilization of Au on freestanding ZrO_2 thin films was observed on O-top site with an adsorption energy of -0.54 eV. Here, Au bound to O surface with a distance of 2.34 Å (Table 1 and Fig 2c).

In all Au adsorption sites on freestanding ZrO_2 thin film, the charge transfer from support to adsorbed Au atom is not observed. This is demonstrated by analyzing the Bader charge of 0 |e|, the spin density of Au (transparent yellow), and the density of the state in which Au still keeps the atomic valence configuration of $6s^1$ as illustrated in Fig 2. The present observation is in good agreement with the previous studies on freestanding reducible ZnO thin films [26] and non-reducible MgO thin films [27].

Considering Au on ZrO_2/Pt_3Zr, the same order of stabilization of Au adsorption configuration was found when placing Au on ZrO_2/Pt_3Zr thin film compared to that on freestanding ZrO_2 thin film.

However, a much stronger adsorption energy was found for Au on the hollow site with an energy gain of -1.28 eV compared to the corresponding site on freestanding ZrO_2 (-0.8 eV) (Table 1 and Fig 2d). Similar distances between Au and Zr (3.00 Å); Au and O (2.85 Å) are found in this configuration compared to that on freestanding ZrO_2 thin film. On the Zr-top site, the Au bound to Zr with an energy of -0.97 eV and a distance of 2.71 Å (Table 1 and Fig 2e). This is 0.37 eV less stable than on hollow site but 0.2 eV much more stable than on the same site on freestanding ZrO_2. In the last case, Au adsorption on O-top site is the least stable with an adsorption energy of -0.29 eV and with a distance of 2.29 Å (Table 1, Fig 2f).

Table 1: Characteristics of Au atom adsorbed on freestanding ZrO_2 and ZrO_2/Pt_3Zr

Au site	ΔE_{ad}[a] (eV)	μB[b]	Q[c] |e|	r(Au-Zr)[d] (Å)	r(Au-O)[e] (Å)	Fig.
			Freestanding ZrO_2			
Hollow	-0.80	1.00	-0.07	3.18	2.66	2a
Zr-top	-0.77	1.00	0.00	2.92	-	2b
O-top	-0.54	1.00	-0.04	-	2.34	2c
			ZrO_2/Pt_3Zr			
Hollow	-1.28	0.00	-0.55	3.00	2.85	3a
Zr-top	-0.97	0.09	-0.48	2.71		3b
O-top	-0.29	0.99	-0.04		2.29	3c

[a]Adsorption energy, [b]magnetization of Au; [c]Bader charge of Au, [d]the shortest distance of Au to Zr surface of ZrO_2, [e]the shortest distance of Au to O surface of ZrO_2.

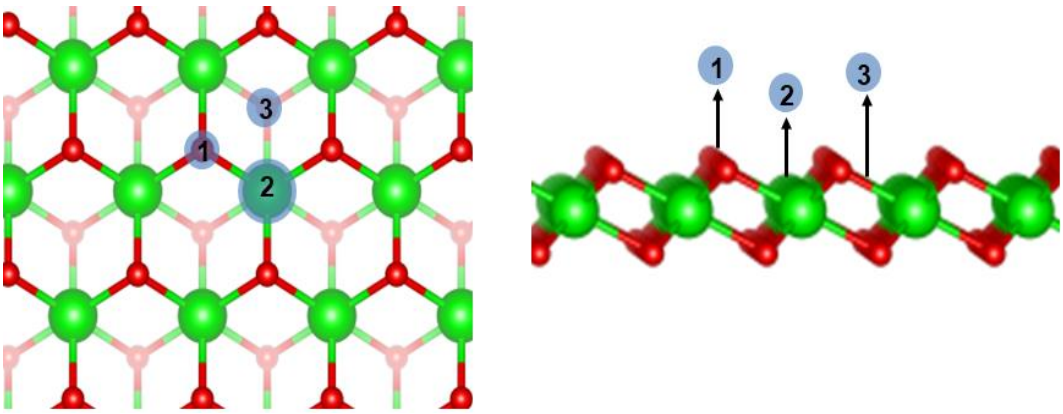

Fig 1: Top view (left), side view (right) of (1) O-top, (2) Zr-top, and (3) hollow sites on ZrO_2 thin film, Zr and O are green and red spheres, respectively

https://doi.org/10.62239/jca.2024.009

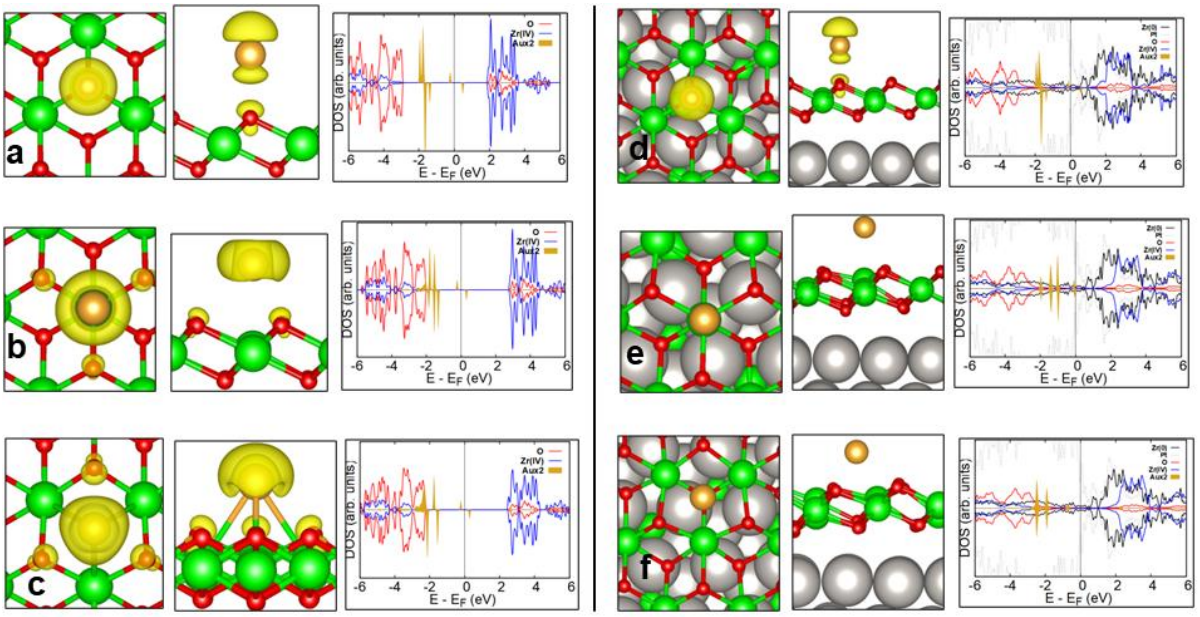

Fig 2: Top view (left), side view (middle), and DOS profile (right) of (a) Au on hollow, (b) Zr-top, and (c) O-top sites of freestanding ZrO_2 , (d) Au on hollow, (e) Zr-top, and (f) O-top sites of ZrO_2 /Pt_3Zr accompanied with spin density. Zr, O, Au, and Pt are green, red, gold, and grey spheres, respectively. Spin density (transparent yellow) was plotted with an isosurface of 0.05 |e|/$Borh^3$

The driven force causing the significant difference in Au adsorption on ZrO_2/Pt_3Zr compared to those on freestanding ZrO_2 thin film is the charge transfer from support to Au. This phenomenon was found for Au on hollow and Zr-top sites as demonstrated by the quenched magnetization of Au, and the negative charge of Au (Bader charge of -0.5 |e|) (Table 1). Furthermore, the charge transfer was confirmed by evaluating spin density and the density of state (Fig 2d-f). In particular, the spin density is completely disappeared and density of state indicates the Au atomic valence configuration of $6s^2$. These results are in line with the previous study of Au on ZnO/Cu(111) [26]. On the other hand, the same observation for Au on the O-top site as compared to Au on freestanding ZrO_2, where Au atomic valence configuration remains as $6s^1$ as gas Au atom, indicated by the magnetization of 1 μB, spin density and DOS profile (Table 1 and Fig 2f).

H_2 adsorption on freestanding ZrO_2 and ZrO_2/Pt_3Zr thin films

H_2 dissociation is mainly found as an important step forward hydrogenation of CO_2 on ZrO_2 thin film via HCOOH path [28]. Therefore, we consider H_2 dissociation on freestanding ZrO_2 and supported ZrO_2 thin films via two mechanisms, homolytic and heterolytic dissociation. The characteristics of H_2 dissociative adsorption are reported in Table 2 and illustrated in Fig 3.

On freestanding ZrO_2 thin films, H_2 dissociation is largely endothermic process with energy cost of 3.18 eV and 1.54 eV for homolytic and heterolytic processes, respectively. For the homolytic dissociation, two extra electrons result from homolytic process localized at Zr^{4+} cations neighboring, in which H bound to O with a bond length of 0.97 Å. This results in reducing Zr^{4+} to Zr^{3+} which is demonstrated by DOS profile and spin density, Fig 3a and the magnetization of 2 (Table 2). On the other hand, the heterolytic dissociation gives rise to H^+ bound to O forming OH group with O-H bond length of 0.97 Å and H^- bound to Zr forming ZrH^- group with Zr-H bond length of 1.90 Å. This is confirmed by Bader charge of H ions bound to O and to Zr of 0.67 |e| and -0.51 |e|, respectively (Table 2) and further indicated by DOS (Fig 3b).

A significant difference was found when H_2 dissociated on ZrO_2/Pt_3Zr thin film compared to that on freestanding ZrO_2 thin film. While homolytic process is exothermic with an energy gain of -0.92 eV, the heterolytic mechanism is endothermic with an energy cost of 0.40 eV, which is about 1 eV smaller than the corresponding process on

https://doi.org/10.62239/jca.2024.009

freestanding ZrO_2 thin film. However, the bond length of O-H (0.97 Å) and Zr-H (1.9 Å) of OH^+ and ZrH^- groups, respectively remain the same as on freestanding ZrO_2 thin films. The main reason causing the difference in the homolytic dissociation of H_2 on ZrO_2/Pt_3Zr with respect to freestanding ZrO_2 thin film is the extra charge transfers to Pt_3Zr support, while the extra charge localized on the freestanding ZrO_2 film. This is demonstrated by the quenched magnetization and illustrated by the DOS and the disappearance of the spin density of ZrO_2 film deposited on Pt_3Zr (Fig 3c-d). These observations are in accordance with those on ZnO thin film deposited on coinage metals [29] and with ZrO_2 thin films deposited on alloy $Pt_3Zr(0001)$, on transition metal Pt(111) [19].

Table 2: Characteristics of H_2 adsorbed on freestanding ZrO_2 and ZrO_2/Pt_3Zr thin film

Mechanism	ΔE_{ad}[a] (eV)	μB[b]	Q[c] |e|	r(H-Zr)[d] (Å)	r(H-O)[e] (Å)	Fig
			Freestanding ZrO_2			
Homolytic	3.18	2.00	0.64; 0.67	-	0.97; 0.97	4a
Heterolytic	1.54	0.00	-0.51; 0.67	1.87	0.97	4b
			ZrO_2/Pt_3Zr			
Homolytic	-0.92	0.00	0.66; 0.65	-	0.97; 0.97	5a
Heterolytic	0.40	0.00	-0.52; 0.64	1.90	0.97	5b

[a]Adsorption energy, [b]magnetization; [c]Bader charge of H, [d]the bond length of H-Zr, [e]the bond length of H-O.

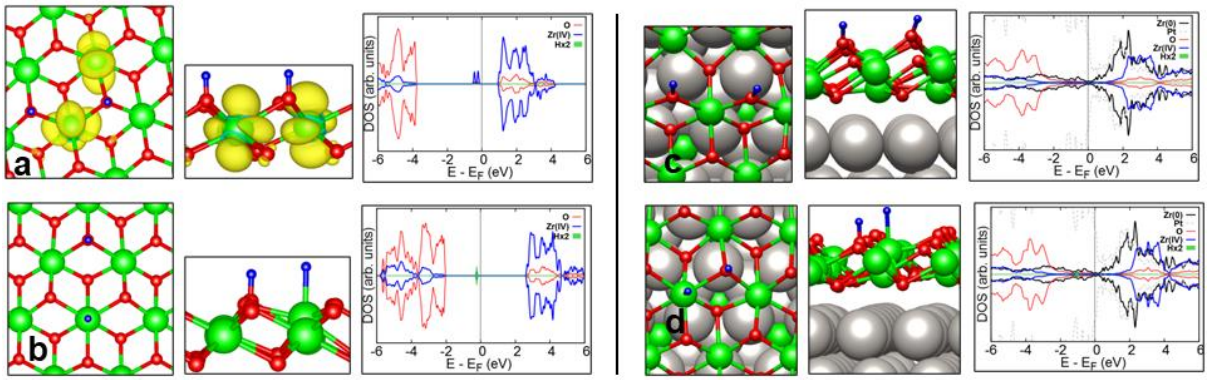

Fig 3: Top view (left), side view (middle), and DOS profile (right) of (a) homolytic dissociation and heterolytic dissociation of H_2 on freestanding ZrO_2 thin film accompanied with spin density; (c) homolytic dissociation and (d) heterolytic dissociation of H_2 on ZrO_2/Pt_3Zr. Zr, O, Pt, and H are green, red, grey, and blue spheres, respectively. Spin density (transparent yellow) was plotted with an isosurface of 0.05 |e|/Borh^3

4. Conclusions

The effect of alloy Pt_3Zr support ZrO_2 thin film on the electronic characteristics of adsorbed Au and H_2 has been investigated by using PBE+U along with dispersion forces. The calculated results present that the Pt_3Zr can act as electron acceptors or donors, which is completely different from those on freestanding ZrO_2 thin film. In particular, the charge transfer from Pt_3Zr to single atom Au leads to negatively charged Au on ZrO_2/Pt_3Zr, while Au atom is neutral on freestanding ZrO_2. Whereas the homolytic dissociation of H_2 is an exothermic process and is preferential on ZrO_2/Pt_3Zr, the heterolytic dissociation is an endothermic process and is preferential on freestanding ZrO_2 film. This study would provide useful information for the application of supported ZrO_2 thin film in catalysis and adsorption.

https://doi.org/10.62239/jca.2024.009

Acknowledgments

This work was supported by The University of Danang, University of Science and Technology, code number of Project: B2022-DN02-17. We are grateful to Prof. Gianfranco Pacchioni for supporting the code.

References

1. E. Fortunato, P. Barquinha, R. Martins, Advances, Adv. Mater. 24 (2012) 2945–2986. https://doi.org/10.1002/adma.201103228.
2. G. Pacchioni, Chem. Eur. J. 18 (2012) 10144–10158. https://doi.org/10.1002/chem.201201117.
3. P. Luches, F. Pagliuca, S. Valeri, J. Phys. Chem. C. 115 (2011) 10718–10726. https://doi.org/10.1021/jp201139y.
4. F. Tumino, C.S. Casari, M. Passoni, C.E. Bottani, A.L. Bassi, Nanotechnology. 27 (2016) 475703. https://doi.org/10.1088/0957-4484/27/47/475703.
5. Y.D. Kim, J. Stultz, D.W. Goodman, Surf. Sci. 506 (2002) 228–234. https://doi.org/10.1016/S0039-6028(02)01386-9.
6. Y. Gao, L. Zhang, Y. Pan, G. Wang, Y. Xu, W. Zhang, J. Zhu, Chin. Sci. Bull. 56 (2011) 502–507. https://doi.org/10.1007/s11434-010-4309-7.
7. G. Pacchioni, L. Giordano, M. Baistrocchi, Phys. Rev. Lett. 94 (2005) 226104. https://doi.org/10.1103/PhysRevLett.94.226104.
8. L. Giordano, G. Pacchioni, J. Goniakowski, N. Nilius, E.D.L. Rienks, H.-J. Freund, Phys. Rev. Lett. 101 (2008) 026102. https://doi.org/10.1103/PhysRevLett.101.026102.
9. H.V. Thang, S. Tosoni, G. Pacchioni, Appl. Surf. Sci. 483 (2019) 133–139. https://doi.org/10.1016/j.apsusc.2019.03.240.
10. K. Li, J.G. Chen, ACS Catal. 9 (2019) 7840–7861. https://doi.org/10.1021/acscatal.9b01943.
11. [G. Pacchioni, ACS Catal. 4 (2014) 2874–2888. https://doi.org/10.1021/cs500791w.
12. H. Li, J.-I.J. Choi, W. Mayr-Schmölzer, C. Weilach, C. Rameshan, F. Mittendorfer, J. Redinger, M. Schmid, G. Rupprechter, J. Phys. Chem. C. 119 (2015) 2462–2470. https://doi.org/10.1021/jp5100846.
13. H. Li, C. Rameshan, A.V. Bukhtiyarov, I.P. Prosvirin, V.I. Bukhtiyarov, G. Rupprechter, Surf. Sci. 679 (2019) 139–146. https://doi.org/10.1016/j.susc.2018.08.028.
14. G. Kresse, J. Furthmüller, Comput. Mater. Sci. 6 (1996) 15–50. https://doi.org/10.1016/0927-0256(96)00008-0.
15. G. Kresse, J. Furthmüller, Phys. Rev. B. 54 (1996) 11169–11186. https://doi.org/10.1103/PhysRevB.54.11169.
16. G. Kresse, D. Joubert, Phys. Rev. B. 59 (1999) 1758–1775. https://doi.org/10.1103/PhysRevB.59.1758.
17. J.P. Perdew, K. Burke, M. Ernzerhof, Phys. Rev. Lett. 77 (1996) 3865–3868. https://doi.org/10.1103/PhysRevLett.77.3865.
18. S.L. Dudarev, G.A. Botton, S.Y. Savrasov, C.J. Humphreys, A.P. Sutton, Phys. Rev. B. 57 (1998) 1505–1509. https://doi.org/10.1103/PhysRevB.57.1505.
19. A.R. Puigdollers, G. Pacchioni, Nanoscale. 9 (2017) 6866–6876. https://doi.org/10.1039/C7NR01904A.
20. G. Teufer, Acta Cryst. 15 (1962) 1187–1187. https://doi.org/10.1107/S0365110X62003114.
21. S. Grimme, J. Comput Chem. 27 (2006) 1787–1799. https://doi.org/10.1002/jcc.20495.
22. S. Tosoni, J. Sauer, Phys. Chem. Chem. Phys. 12 (2010) 14330–14340. https://doi.org/10.1039/C0CP01261K.
23. E. Sanville, S.D. Kenny, R. Smith, G. Henkelman, J. Comput. Chem. 28 (2007) 899–908. https://doi.org/10.1002/jcc.20575.
24. W. Tang, E. Sanville, G. Henkelman, J. Phys.: Condens. Matter. 21 (2009) 084204. https://doi.org/10.1088/0953-8984/21/8/084204.
25. M. Yu, D.R. Trinkle, J. Chem. Phys. 134 (2011) 064111. https://doi.org/10.1063/1.3553716.
26. H.V. Thang, S. Tosoni, G. Pacchioni, ACS Catal. 8 (2018) 4110–4119. https://doi.org/10.1021/acscatal.7b03896.
27. M. Yulikov, M. Sterrer, M. Heyde, H.-P. Rust, T. Risse, H.-J. Freund, G. Pacchioni, A. Scagnelli, Phys. Rev. Lett. 96 (2006) 146804. https://doi.org/10.1103/PhysRevLett.96.146804.
28. C. Wu, L. Lin, J. Liu, J. Zhang, F. Zhang, T. Zhou, N. Rui, S. Yao, Y. Deng, F. Yang, W. Xu, J. Luo, Y. Zhao, B. Yan, X.-D. Wen, J.A. Rodriguez, D. Ma, Nat Commun. 11 (2020) 5767. https://doi.org/10.1038/s41467-020-19634-8.
29. H.V. Thang, G. Pacchioni, ChemNanoMat. 5 (2019) 932–939. https://doi.org/10.1002/cnma.201900195.